Nuclear Inst. and Methods in Physics Research, A 1053 (2023) 168381

Contents lists available at ScienceDirect

Nuclear Inst. and Methods in Physics Research, A

journal homepage: www.elsevier.com/locate/nima

Full Length Article

Achieving significant performance recovery of SiPMs' irradiation damage with in-situ current annealing

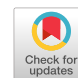

Fengbo Gu [a], Yaqing Liu [b,d], Xilei Sun [b,c,*], Yanbing Xu [b,d,*], Dali Zhang [b,d], Zhenghua An [b,d], Ke Gong [b,d], Xinqiao Li [b,d], Xiangyang Wen [b,d], Shaolin Xiong [b,d], Fan Zhang [b,d], Chenger Wang [e], Guopu Qu [a,**]

[a] School of Nuclear Science and Technology, University of South China, Hengyang, 421001, Hunan, China
[b] Institute of High Energy Physics, Chinese Academy of Sciences (CAS), Beijing, 100049, China
[c] State Key Laboratory of Particle Detection and Electronics, Institute of High Energy Physics, Chinese Academy of Sciences (CAS), Beijing, 100049, China
[d] Key Laboratory of Particle Astrophysics, Institute of High Energy Physics, Chinese Academy of Sciences (CAS), Beijing, 100049, China
[e] National Engineering Research Center for Rare Earth Materials, General Research Institute for Nonferrous Metals, Beijing, 100088, China

ARTICLE INFO

Keywords:
SiPM
Irradiation damage
Dark current
In-situ annealing

ABSTRACT

Irradiation damage is one of the main drawbacks restricting the application of Silicon Photomultiplier (SiPM), especially in high irradiance environments such as space, colliders, and nuclear power plants. In-situ current annealing is a method of using the self-current heating of SiPM, and because it does not require disassembly of the SiPM and additional heating devices, it exhibits potential for dealing with radiation damage. We investigate the in-situ annealing performance of three types of SiPM for irradiation damage. The annealing current and time are optimized and the SiPM performance before and after annealing is compared. It was found that after annealing the dark currents of the three types of SiPMs decreased significantly by 1–2 orders of magnitude. Finally, the variation of SiPM performance with temperature is investigated. The energy resolution does not recover as well as the dark current.

1. Introduction

Silicon photomultiplier tubes (SiPMs) are considered novel semiconductor photodetectors. Owing to their small size, high gain, high photon detection efficiency, and low operating voltage, they have gradually become the first choice for photoelectric detection [1], especially in space microsatellite applications [2]. However, a major disadvantage of SiPMs is that they are easily damaged in complex irradiation environments [3–5], resulting in performance deterioration and reduced operating life. Extensive studies have shown that there are two main types of radiation damage in SiPM, namely ionization damage and displacement damage. The ionizing damage affects the performance below the breakdown voltage [6–8]. Displacement damage is caused by lattice defects that result from the collision of high-energy particles such as protons and neutrons with Si nuclei [9,10]. Previous studies have reported that displacement damage mainly results in a decrease in the output signal amplitude, manifested as a decrease in gain due to displacement damage, and is mainly observed for irradiance flux [11], an increase in dark current [12], and a decrease in the photon detection efficiency (PDE) [13]. The GECAM [14] satellite developed in-house by our research group has detected obvious SiPM radiation damage in orbit. Therefore, the recovery of radiation damage of SiPM needs to be studied and solved urgently. Annealing is a well-established method for addressing SiPM performance recovery against radiation damage. It has previously been observed that long-time annealing at both room temperature [15–17] and a high temperature [18–21] can effectively restore the performance of SiPM. A special annealing method is in-situ current annealing, in which a current is applied to the SiPM, and the current heats the SiPM to achieve a high-temperature annealing effect [22,23]. This method does not require the disassembly of the SiPM or additional heating devices and can be realized through circuit design, hence it is especially suitable for space applications or colliders and other situations where replacement and maintenance are difficult. Previous studies have shown that the presence of a strong electric field also plays a role in annealing [24]. In this study, we investigated three types of SiPM by in-situ annealing, which are SensL MicroFJ-60035-TSV [25], Hamamatsu S14160-3010PS [26], and NDL EQR1511-3030D-S [27].

* Corresponding authors at: Institute of High Energy Physics, Chinese Academy of Sciences (CAS), Beijing, 100049, China.
** Corresponding author.
E-mail addresses: sunxl@ihep.ac.cn (X. Sun), xuyb@ihep.ac.cn (Y. Xu), quguopu@usc.edu.cn (G. Qu).

https://doi.org/10.1016/j.nima.2023.168381
Received 4 January 2023; Received in revised form 9 May 2023; Accepted 15 May 2023
Available online 29 May 2023
0168-9002/© 2023 Elsevier B.V. All rights reserved.

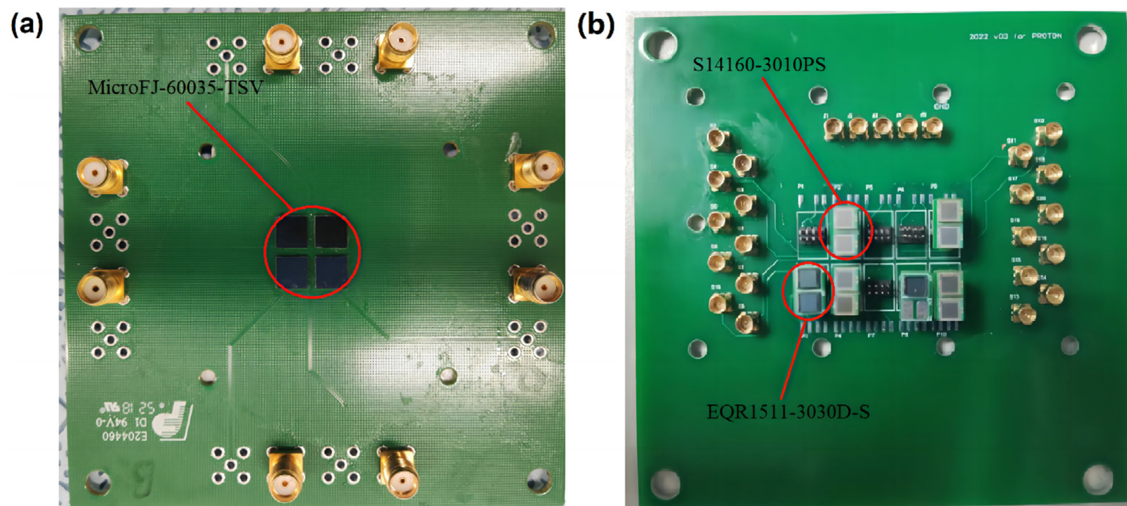

Fig. 1. The test circuit boards, (a) SensL MicroFJ-60035-TSV, (b) Hamamatsu S14160-3010PS, and NDL EQR1511-3030D-S.

Table 1
Irradiation fluence for SiPMs.

Manufacturer	Beam flow type	Sample	Model	φ_{eq} (n_{eq}/cm^2)
SensL	Proton	A	MicroFJ-60035-TSV	2.7×10^8
		B		2.7×10^9
		C		4.6×10^{10}
Hamamatsu	Neutron	D	S14160-3010PS	1.0×10^9
		E		1.0×10^{10}
		F		1.0×10^{12}
NDL	Neutron	G	EQR15 11-3030D-S	1.0×10^{10}

2. Experimental set-up

2.1. Irradiation of SiPMs

The test circuit boards of the SiPMs are shown in Fig. 1, and the SensL MicroFJ-60035-TSV chip is 6 mm × 6 mm with a 35 μm pitch as shown in Fig. 1(a), Hamamatsu S14160-3010PS is 3 mm × 3 mm with a 10 μm pitch and NDL EQR1511-3030D-S is 3 mm × 3 mm with a 15 μm pitch as shown in Fig. 1(b). The beam spot covered the SiPM area of each board, and there were multiple test plates, each of which received one dose of radiation.

The SensL MicroFJ-60035-TSV SiPMs were irradiated at the Chinese Institute of Atomic Energy (CIAE) using the HI-13 tandem accelerator [28] on April 13 2021. The 19 MeV proton beam was used to irradiate SiPM from 10^8 to 10^{10} proton/cm^2 at a flux rate of 5~10 × 10^7 counts/cm^2/s. A Keithley 6517 picometer was used to monitor changes in dark current during irradiation. The Hamamatsu S14160-3010PS and NDL EQR1511-3030D-S SiPMs were irradiated at the China Spallation Neutron Source on 8 July 2022 by using ES#2 spot [29]. The neutron beam was used to irradiate SiPM from 10^9 to 10^{12} neutron/cm^2 at a flux rate of 6.9 × 10^6 counts/cm^2/s. SensL has 12 SiPMs, with every four pieces grouped together and soldered onto a single test board, as shown in Fig. 1(a). Hamamatsu has six SiPMs, with every two pieces grouped together and each group receiving a single dose of radiation. NDL has two SiPMs grouped together and receiving a single dose of radiation. The displacement damage caused by different charged particles on the semiconductor varies. Globally, to study the displacement damage caused by different particles, the radiation particle flux will be converted into a 1 MeV neutron injection [30]. The equivalent 1 MeV neutron fluence [31] is shown in Table 1.

2.2. Annealing methods of SiPM

SiPM in-situ annealing was performed by heating it with a forward current flowing from the anode to the cathode. The concept diagram of the equipment is shown in Fig. 2. The SiPM was placed in a dark box, the constant current source was Keithley 2450, and the temperature measuring instrument was a Fluke TiS55+ infrared thermometer. Different annealing effects can be achieved by varying different currents and times, but to prevent damage to the SiPM maximum heating temperature should not exceed the chip reflow temperature of 260 °C. The annealing current of SensL MicroFJ-60035-TSV SiPM was 0.5 A, 0.6 A, 0.7 A, and 0.8 A for the same group of four different SiPMs respectively, and the annealing time was the shortest 10 s and the longest 1800 s. Hamamatsu S14160-3010PS and NDL EQR1511-3030D-S SiPMs were annealed at a current of 0.8 A for 100 s. Room temperature annealing was performed for eight months before the in-situ current annealing of SensL MicroFJ-60035-TSV SiPMs. After each annealing, a half-hour cooling period was necessary to ensure sufficient cooling and to prevent an increase in dark current caused by inadequate cooling. The testing after annealing is conducted at room temperature, which is 20 °C when cooled down.

2.3. SiPMs performance test

The Keithley 6517 picometer was used to measure the dark current of each SiPM. All SiPMs were placed in cryogenic bins for dark current testing as shown in Fig. 3. Unless otherwise noted, all measurements in this study were performed at fixed operating voltages and at room temperature. In particular, cooling to room temperature is required for dark current measurements after annealing. SensL SiPM was performed using a SiPM bias voltage of 28.0 V, which corresponds to a 3.5 V overvoltage. Hamamatsu SiPM was performed using a SiPM bias voltage of 43.0 V, which corresponds to a 5.0 V overvoltage. NDL SiPM was performed using a SiPM bias voltage of 38.0 V, which corresponds to an 8.0 V overvoltage. The overvoltage we used was determined by employing the breakdown voltage stated in the data sheet. The MicroFJ-60035-TSV SiPM was used as a photo-detector to detect the γ-ray from the dotted ^{137}Cs radioactive source. The experimental set-up includes a $LaBr_3$ crystal, the GECAM ground detection data acquisition system, a high and low temperature experimental box, and a ^{137}Cs radioactive source. The GECAM ground test system is a device for testing satellite systems under ground control. It has a sampling rate of 40 M/s and eight acquisition channels, and can provide a stable voltage

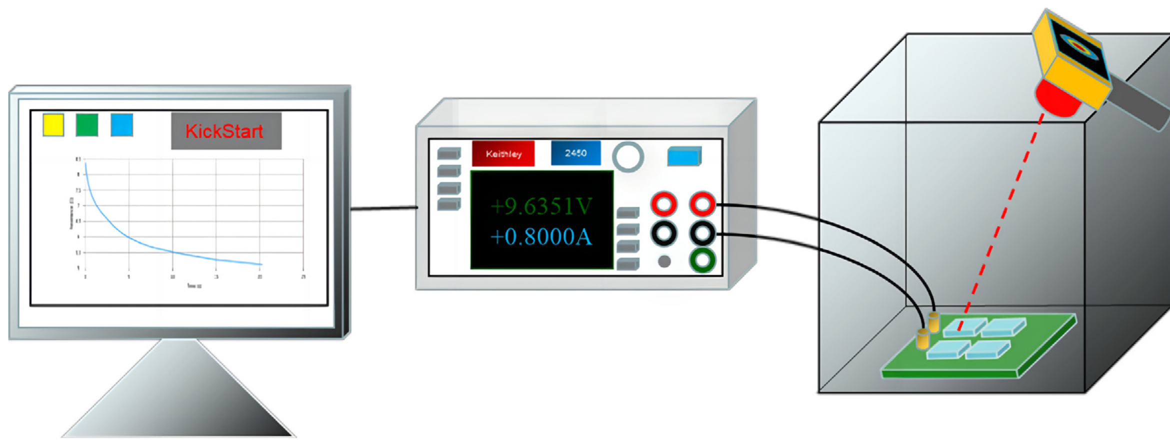

Fig. 2. The concept diagram of the in-situ annealing device.

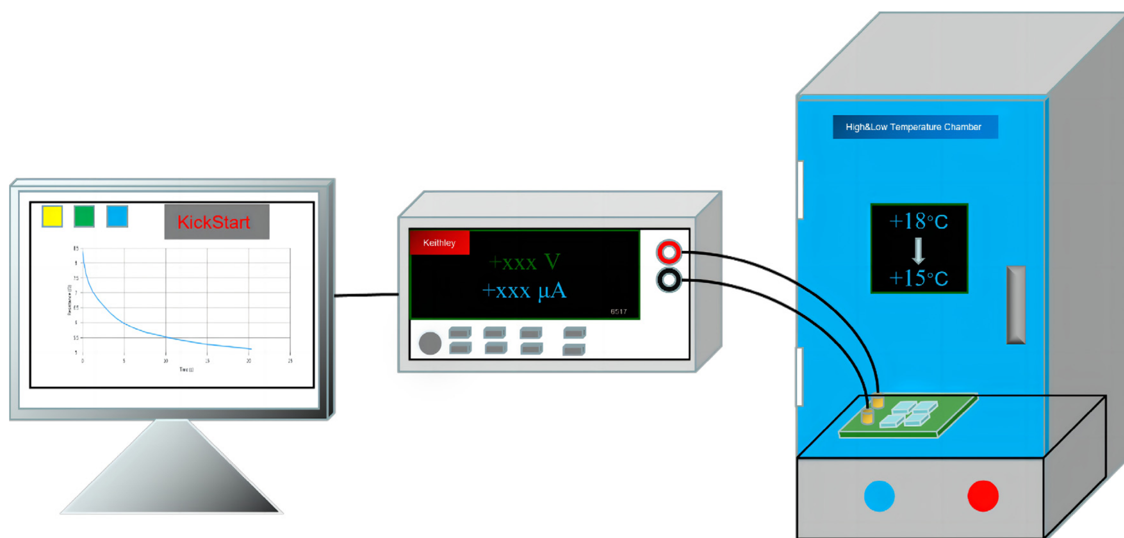

Fig. 3. The concept diagram of the low-temperature test device.

of about 28 V. It contains differential circuits that can filter out noise. For comparison, the full energy peak for the dotted ^{137}Cs radioactive source was measured before and after irradiation and after annealing for comparison.

3. Results and discussion

3.1. Annealing

The variation of MicroFJ-60035-TSV SiPM dark current with equivalent neutron fluence is shown in Fig. 4. Usually, the SiPM dark current is proportional to the radiation dose. The nonlinearity of the current growth is caused by the instability of the proton beam, and the plateau area at the top is caused by the saturation of the Picometer. The dark current in the figure increases slowly than expected as the delivered radiation dose increases. One possible reason is that SiPM has a self-annealing effect at room temperature. Similar results are shown in Ref. [32]. The three types of SiPM used in this study are SensL SiPM with different fluence values: A (2.7×10^8), B (2.7×10^9) and C (4.6×10^{10}). The current value corresponding to a 28.0 V bias voltage measured immediately after irradiation and maintaining it at room temperature for eight months are shown in Table 2. The 28.0 V dark current without irradiation is ~2 μA, and it can be seen that the dark current increased by 20, 211, and 4000 times for these three different doses, respectively. After eight months, their dark currents were all

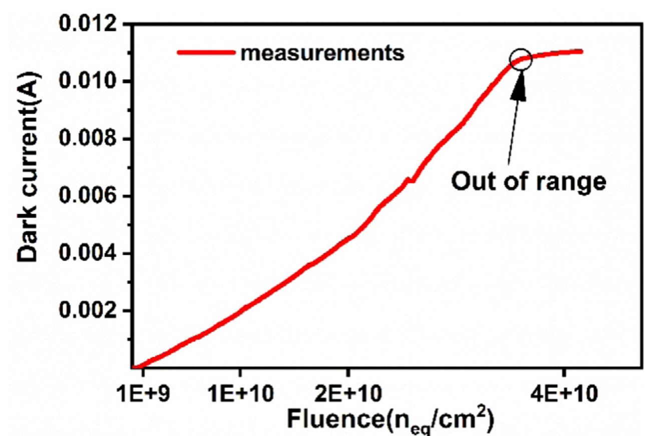

Fig. 4. Plot of the dark current of MicroFJ-60035-TSV SiPM at an operating voltage of 28.0 V as a function of the equivalent neutron fluence of the 19 MeV proton injection.

reduced by more than 60%, this obvious room temperature annealing effect is consistent with the literature [33].

The dark current values of SiPM with an irradiation injection of 4.6×10^{10} n_{eq}/cm^2 in Table 2 are different from the one in Fig. 4. This

Table 2
Results of SiPM dark current measured immediately after irradiation.

SiPM samples	φ_{eq} (n_{eq}/cm^2)	Dark current (μA)	
		After irradiation	After annealing at room temperature for eight months
A	2.7×10^8	40.0	14.8
B	2.7×10^9	423.0	158.7
C	4.6×10^{10}	7917.5	3028.5
D	1.0×10^9	0.6	–
E	1.0×10^{10}	5.4	–
F	1.0×10^{12}	530.0	–
G	1.0×10^{10}	81.1	–

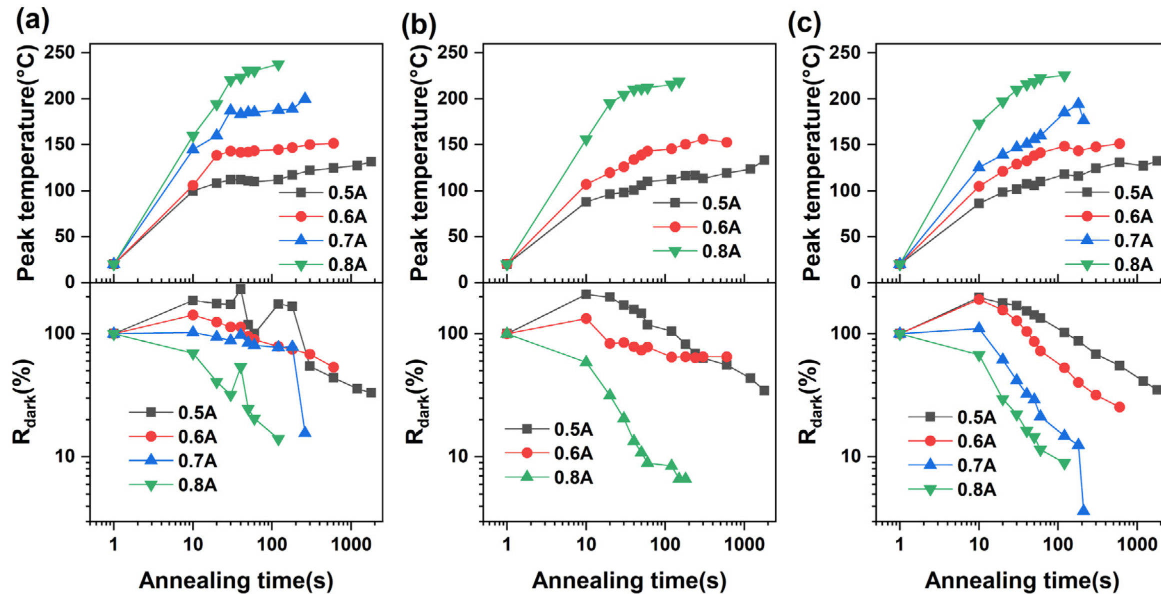

Fig. 5. Maximum temperature at each annealing (top) and dark current of MicroFJ-60035-TSV SiPM with an operating voltage of 28.0 V after each annealing (bottom). (a), (b) and (c) denote SiPM with irradiation fluence 2.7×10^8 n_{eq}/cm^2, 2.7×10^9 n_{eq}/cm^2, and 4.6×10^{10} n_{eq}/cm^2, respectively.

abnormal result of the SiPM dark current after the third exposure was due to SiPM self-heating when the SiPM dark current is 7.9 mA. The radiation doses of SiPM in groups D, E, and F are respectively 1.0×10^9 n_{eq}/cm^2, 1.0×10^{10} n_{eq}/cm^2 and 1.0×10^{12} n_{eq}/cm^2. The 43.0 V dark current of S14160-3010PS SiPM without irradiation is ∼0.03 μA, it can be seen that dark current increased by 20, 181, and 17 667 times for these 3 different doses, respectively. The radiation doses of SiPM in group G is 1.0×10^{10} n_{eq}/cm^2. The 38.0 V dark current of EQR15 11-3030D-S SiPM without irradiation is ∼0.2 μA, it can be seen that for this dose, the dark current increased by a factor of 40 times.

After maintaining it at room temperature for eight months, we performed current annealing experiments on these MicroFJ-60035-TSV SiPMs. The relationship between the annealing temperature, relative change of dark current and annealing time is shown in Fig. 5. From the experimental results, it can be seen that the annealing temperature increased as the current and annealing time increased, and the annealing temperature entered a plateau region with slow growth when the annealing time extends to about 30 s. The ratio of the dark current after annealing to that before annealing is defined as R_{dark}. The reference current used to define R_{dark} is the current measured after annealing at room temperature for eight months prior to current annealing. From its variation with annealing time, we observed that the dark current increased significantly at lower annealing temperatures(under 150 °C) or shorter annealing times, indicating a deterioration of device performance. Therefore, proper annealing conditions are crucial for optimizing device performance.

We used a gradual increase in annealing time, that is, the annealing time before each measurement is an accumulation of the previous one. For example, the annealing time before the second measurement is 10 s plus 20 s, the annealing time before the third measurement is 10 s plus 20 s plus 30 s, and so on. Therefore, it is reasonable for the peak temperature in Fig. 5 to increase with the annealing time. After annealing for 120 s using a current of 0.8 A, the peak temperature reached 220 °C–235 °C, and the dark currents of the three groups of SiPMs decreased to 14%, 10%, and 8% of the pre-annealing values, respectively. It should be noted that the dark current fluctuation corresponding to 0.5 A in Fig. 5(a) (bottom) may be caused by light leakage from the dark box during the test. In Fig. 5(b) (bottom), the missing 0.7 A annealing result is due to a piece of SiPM that was damaged during the lab placement. A general trend is that the larger the current and the longer the time, the better is the annealing effect, and when the annealing time reaches 100 s, the dark current enters a slowly changing plateau region. According to the experimental results, 0.8 A current has the best annealing effect, and the temperature does not exceed the reflow temperature of SiPMs, so the following two groups of experiments are carried out with 0.8 A current.

The 0.8 A current annealing results of S14160-3010PS SiPM are shown in Fig. 6. After annealing for 20 s, the peak temperature rises to 248 °C, and the dark currents of the three groups of SiPMs drop to 6%, 3%, and 1% of the pre-annealing values, respectively. This is related to the different sensors, because the results show that Hamamatsu can reach a higher temperature in a shorter time using the same annealing current, which leads to a larger dark current drop. We believed that this is related to the quenching resistance, where the larger the quenching resistance, the more heat will be generated by the circuit through the same current at the same time, so the higher the temperature, the lower the dark current drop.

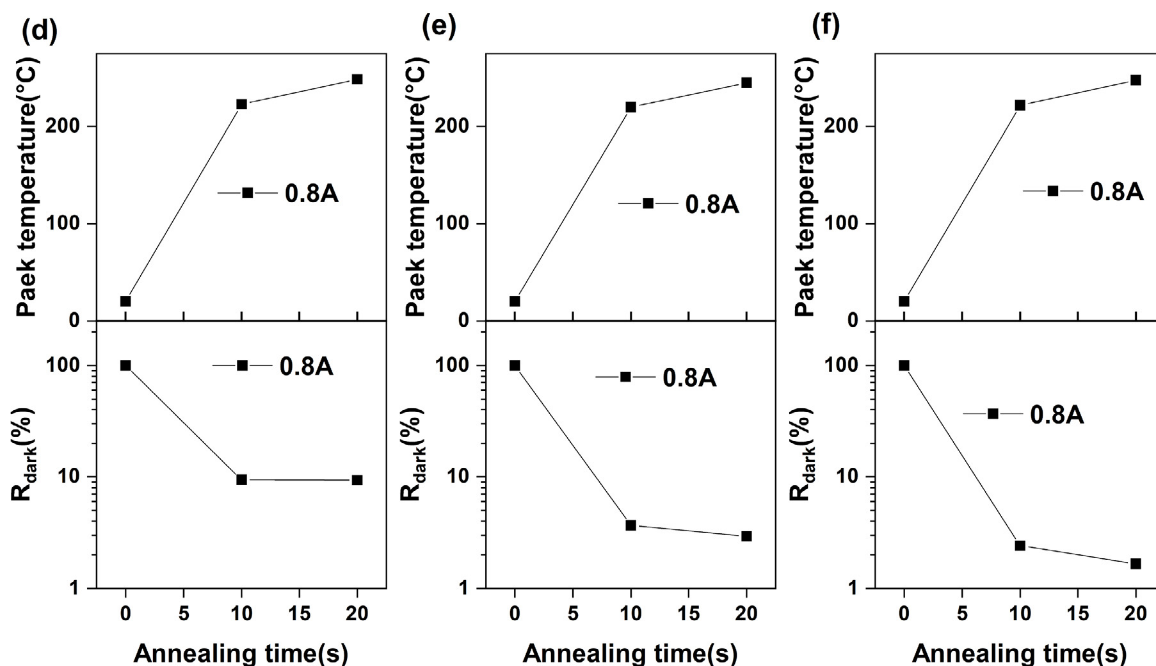

Fig. 6. Maximum temperature at each annealing (top) and dark current of S14160-3010PS SiPM with an operating voltage of 43.0 V after each annealing (bottom). (a), (b) and (c) denote SiPM with irradiation injections of 1.0 × 10^9 n_{eq}/cm^2, 1.0 × 10^{10} n_{eq}/cm^2, and 1.0 × 10^{12} n_{eq}/cm^2, respectively.

The 0.8 A current annealing results of EQR15 3030D SiPM are shown in Fig. 7. After annealing for 150 s, the peak temperature rises to 248 °C, and the dark current decreases to 0.9% of the pre-annealing value.

The decreases of the dark current values of the eight groups of SiPMs after in-situ current annealing using a 0.8 A current are summarized in Fig. 8. Three kinds of SiPM from different manufacturers undergo current annealing after irradiation, and the dark current decreases by 1–2 orders of magnitude.

3.2. Low temperature performance

Low temperature can effectively reduce the dark current, so we tested the effect of low temperature on the dark current before irradiation, after irradiation and after annealing. The dark currents of SensL MicroFJ-60035-TSV, Hamamatsu S14160-3010PS, and NDL EQR15 3030D SiPMs at different temperatures are shown in Figs. 9(top), 9(middle), and 9(bottom), respectively. It can be seen from the figure that the dark currents of all eight groups of SiPMs decrease with decreasing temperature. The peak temperature of SiPMs in Fig. 9 during annealing is within the temperature range of 220 °C–248 °C, as shown in Figs. 5, 6, and 7. One point to note is that we measured the temperature dependence at a constant voltage, and the constant bias actually comes from the conditions of the microsatellite platform. Due to limited resources, the microsatellite platform finds it difficult to adjust the SiPM bias with temperature changes, and generally a fixed bias power supply is used. Therefore, the temperature dependence measurements in this paper are all conducted at a fixed bias. The reason why the lowest temperature is set to −30 degrees is also based on the temperature of the microsatellite, the general microsatellite has no temperature control, and the lowest temperature can reach −30 degrees. Of course, in fact, cooling will reduce the breakdown voltage of the SiPM, maintaining a constant voltage actually increases the overvoltage of the SiPM, which will lead to an increase in the dark count. Meanwhile, cooling also has the effect of suppressing the dark count, this is a complex process with multiple variables coupled together.

The test results of the energy resolution are shown in Fig. 10. In Fig. 10, the peak temperature of SiPMs during annealing is also within the range of 220 °C and 235 °C, as demonstrated in Fig. 5. No significant change in energy resolution is shown in Fig. 10(a) and (b). As the temperature decreases, the energy resolution of the irradiated SiPM in Fig. 10(c) is significantly decreased. In-situ current annealing of the irradiated SiPM shows a significant improvement in the energy resolution of the SiPM at high irradiation injection. As shown in the figure, after annealing, the energy resolution did not improve with temperature variation for all radiation doses.

The peak position of the 662 keV peak of ^{137}Cs was measured every 5 °C between −30 °C and 20 °C, as shown in Fig. 11. Similarly, the peak temperature of SiPMs during annealing in Fig. 11 is between 220 °C–235 °C, as indicated in Fig. 5. Comparing the results, it can be seen that the peak positions of 662 keV in all three groups of SiPM decreased to different degrees after irradiation compared with the peak positions before irradiation. Among them, the peak position of the irradiation injection of 4.6 × 10^{10} n_{eq}/cm^2 has the largest decrease of about 40%, as shown in Fig. 11(c). After in-situ current annealing, the peak positions of the 662 keV peaks obtained from all three groups of SiPM test ^{137}Cs recovered to about 80% of the pre-irradiation levels.

The energy resolution is also related to the bias voltage of the SiPM, so we tested the detector energy resolution of the SiPM with different irradiation doses separately. The results of energy resolution as a function of voltage are shown in Fig. 12. The best operating voltage of the SiPM after annealing was obtained based on the energy resolution of 356 keV versus the operating voltage. The energy resolution of 356 keV obtained from the SiPM test is shown in Fig. 12. The SiPM operating voltage is too small or too large voltage will worsen the energy resolution. From the data, there is no significant difference in the optimum operating voltage of each SiPM, which is approximately 28.2 V.

3.3. Discussion

As mentioned above, in-situ current annealing has a significant annealing effect on all three types of SiPM that were subjected to radiation, namely Hamamatsu, NDL, and SENSL SiPMs. As shown in

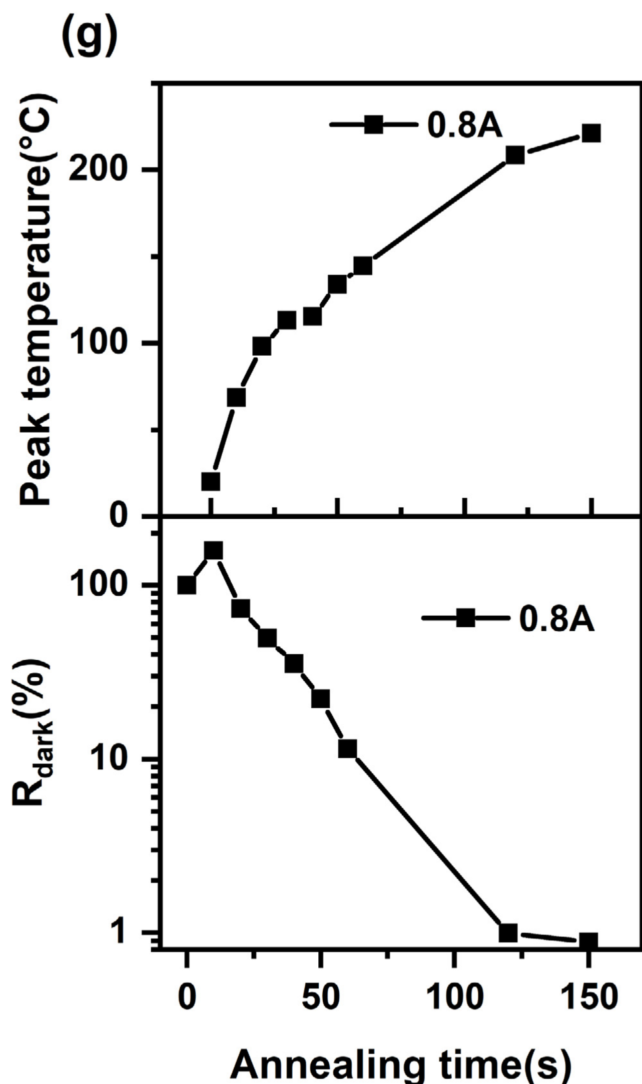

Fig. 7. Maximum temperature at each annealing (top) and dark current of EQR15 3030D SiPM with an operating voltage of 38.0 V after each annealing (bottom). The irradiation fluence of SiPM is 1.0×10^{10} n_{eq}/cm^2.

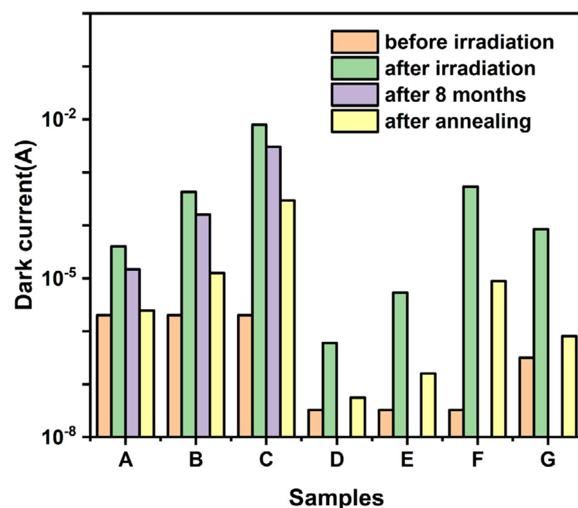

Fig. 8. Dark current of SiPM at 20 °C. The operating voltage is 28.0 V for SensL, 43.0 V for Hamamatsu, and 38.0 V for NDL. The irradiation fluence to each MicroFJ-60035-TSV SiPM Samples A, B and C were 2.7×10^8 n_{eq}/cm^2, 2.7×10^9 n_{eq}/cm^2 and 4.6×10^{10} n_{eq}/cm^2. The irradiation fluence to each S14160-3010PS SiPM Samples D, E and F were 1.0×10^9 n_{eq}/cm^2, 1.0×10^{10} n_{eq}/cm^2 and 1.0×10^{12} n_{eq}/cm^2. The irradiation fluence to EQR15 3030D SiPM Samples G is 1.0×10^{10} n_{eq}/cm^2.

Fig. 5, the annealing effect of different currents on the irradiated SiPM damage varied, with the 0.8 A current providing the best annealing effect. The different annealing times required for different SiPM models are due to the different resistance values of the quenching resistors of the different SiPMs, so the heat production is different for the same current.

Regarding the reduction in the ADC count shown in Fig. 11 after irradiation, it is quite challenging to accurately understand the reason based on the limited experimental data we currently have. We have intuitively speculated several possibilities here: one is due to the reduction of gain, another is due to the reduction of PDE, and another possibility is the joint result of both the gain and PDE reduction. Why the gain and PDE would decrease needs further research. Conclusions reported from Ref. [34] indicate that SiPMs with lower electric fields and higher breakdown voltages have better radiation tolerance, indicating that the SensL sensor used in this study may have weaker radiation tolerance owing to its lower breakdown voltage and higher electric field. The SiPM energy resolution deteriorated with higher irradiation injection in Fig. 10, and similar results were found in [35,36]. One explanation is that in Ref. [37], when the noise level increases after irradiation, some of the APD cells in SiPM are in a dark noise-induced avalanche state and cannot respond to incident light. Several factors may affect the energy resolution of $LaBr_3$ scintillators with temperature, such as the light output of the crystal, the dark noise and correlated avalanche of SiPMs, and the overvoltage applied to SiPMs. According to literature [38,39], the energy resolution of $LaBr_3$ crystal will be slightly improved with a decrease of temperature, which may be counterbalanced by the change of SiPM performance with the increase of overvoltage. In our experiment, we observed that the energy resolution did not change much with temperature within our measurement range (−30–20 °C). This may indicate that these factors have a small or canceling effect on each other under our experimental conditions. The purpose of showing the temperature dependence at constant voltage was to study the effect of temperature on the performance of the detector. However, the changes in performance due to temperature are convoluted and not solely dependent on the data provided in this paper. The low-temperature performance tests showed that although the properties of the SiPMs improved after annealing, they did not fully recover to their pre-irradiation levels. However, SiPM still does not fully recover to its pre-irradiation state after in-situ current annealing.

4. Conclusion

In-situ current annealing tests were performed on three different types of SiPM obtained from SensL, Hamamatsu, and NDL. In the tests, we compared the annealing effect of different currents on SiPM and found that the best in-situ current annealing effect was achieved using a current of 0.8 A. The annealing times required for the three SiPMs using a 0.8 A forward current were 120 s for MicroFJ-60035-TSV, 20 s for S14160-3010PS, and 150 s for EQR15 3030D. For all three different models of SiPMs the dark current decreases with the increase of peak temperature during in-situ current annealing. After the annealing process, the dark current of all SiPMs decreased by 1–2 orders of magnitude. When tested at temperatures of −30 °C–20 °C, it was found that in-situ current annealing fixed the reduced sensitivity of the irradiated SiPM to temperature, improved the energy resolution of the SiPM, and restored the peak position of the SiPM to

Fig. 9. Dark current of SiPMs at different temperatures. The operating voltage is 28.0 V for SensL, 43.0 V for Hamamatsu, and 38.0 V for NDL. The irradiation fluence to MicroFJ-60035-TSV SiPM sample A, B and C was 2.7×10^8 n_{eq}/cm^2, 2.7×10^9 n_{eq}/cm^2 and 4.6×10^{10} n_{eq}/cm^2. The irradiation fluence to each S14160-3010PS SiPM sample D, E and F was 1.0×10^9 n_{eq}/cm^2, 1.0×10^{10} n_{eq}/cm^2 and 1.0×10^{12} n_{eq}/cm^2, respectively. The irradiation fluence to EQR15 3030D SiPM sample G is 1.0×10^{10} n_{eq}/cm^2.

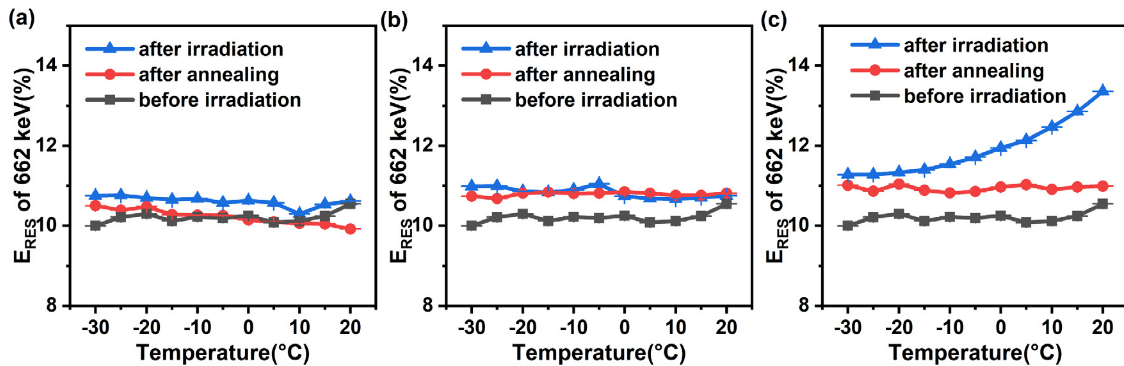

Fig. 10. The energy resolution for ^{137}Cs source as a function of temperature, measured with MicroFJ-60035-TSV SiPMs with an operating voltage of 28.0 V. The irradiation fluence to each MicroFJ-60035-TSV SiPM sample A, B and C was 2.7×10^8 n_{eq}/cm^2, 2.7×10^9 n_{eq}/cm^2 and 4.6×10^{10} n_{eq}/cm^2, respectively.

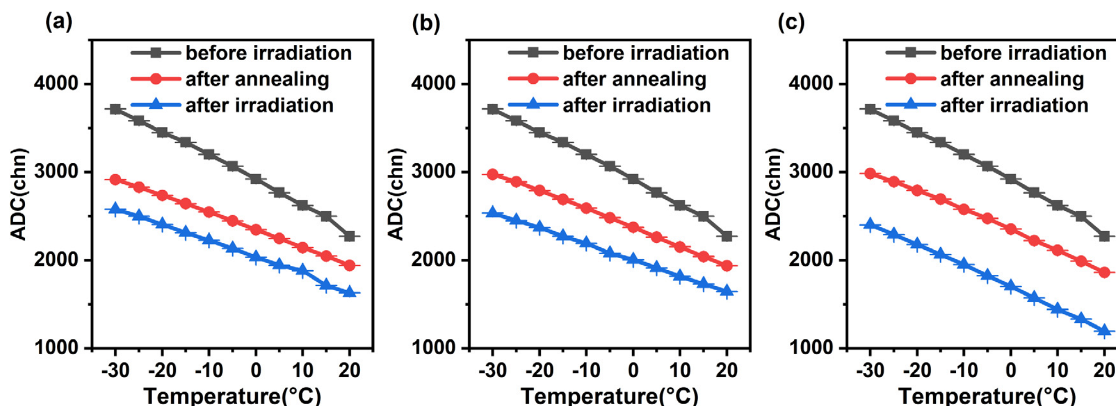

Fig. 11. The peak position for ^{137}Cs source as a function of temperature, measured with MicroFJ-60035-TSV SiPMs with an operating voltage of 28.0 V. The irradiation fluence to each MicroFJ-60035-TSV SiPM Samples A, B and C was 2.7×10^8 n_{eq}/cm^2, 2.7×10^9 n_{eq}/cm^2 and 4.6×10^{10} n_{eq}/cm^2, respectively.

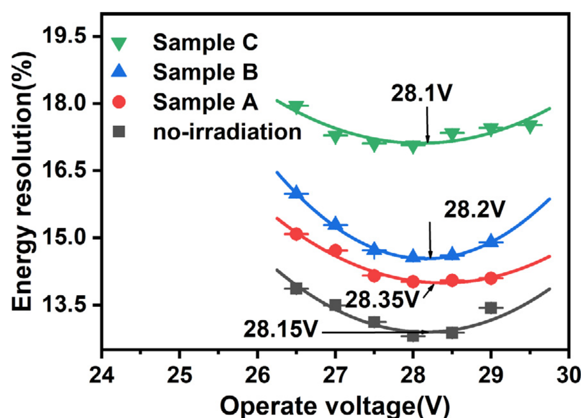

Fig. 12. Best operating voltage determination, based on the best energy resolution of ^{133}Ba source for the SensL MicroFJ-60035-TSV SiPM after annealing at room temperature. The irradiation fluence to each MicroFJ-60035-TSV SiPM sample A, B, and C was 2.7×10^8 n_{eq}/cm^2, 2.7×10^9 n_{eq}/cm^2 and 4.6×10^{10} n_{eq}/cm^2, respectively.

about 80% of its pre-irradiation level. Overall, several properties of SiPM were significantly improved after in-situ current annealing. In conclusion, short-time and high-current in-situ annealing is an effective and convenient SiPM radiation-resistant technical solution.

Declaration of competing interest

The authors declare that they have no known competing financial interests or personal relationships that could have appeared to influence the work reported in this paper.

Data availability

Data will be made available on request.

Acknowledgments

This research was supported by the National Key Research and Development Program of China (Grant No. 2022YFB3503600), the Strategic Priority Research Program of the Chinese Academy of Sciences (Grant No. XDA 15360100, XDA 15360102) and the National Natural Science Foundation of China (Grant No. 211315C10).

References

[1] S. Gundacker, A. Heering, The silicon-photomultiplier: fundamentals and applications of a modern solid-state photon detector, Phys. Med. Biol. (2020).

[2] D. Zhang, X. Li, S. Xiong, Y. Li, X. Sun, Z. An, Y. Xu, Y. Zhu, W. Peng, H. Wang, F. Zhang, Energy response of GECAM gamma-ray detector based on LaBr3:Ce and SiPM array, Nucl. Instrum. Methods Phys. Res. A 921 (2019) 8–13, http://dx.doi.org/10.1016/j.nima.2018.12.032.

[3] B. Biro, G. David, A. Fenyvesi, J.S. Haggerty, J. Kierstead, E.J. Mannel, T. Majoros, J. Molnar, F. Nagy, S. Stoll, B. Ujvari, C.L. Woody, A comparison of the effects of neutron and Gamma radiation in silicon photomultipliers, IEEE Trans. Nucl. Sci. 66 (7) (2019) 1833–1839, http://dx.doi.org/10.1109/tns.2019.2921102.

[4] C. E.Simoen, Radiation Effects in Advanced Semiconductor Materials and Devices, Springer Berlin Heidelberg, 2002.

[5] G. Lindström, Radiation damage in silicon detectors, Nucl. Instrum. Methods Phys. Res. A 512 (1–2) (2003) 30–43, http://dx.doi.org/10.1016/s0168-9002(03)01874-6.

[6] C. Xu, R. Klanner, E. Garutti, W.-L. Hellweg, Influence of X-ray irradiation on the properties of the Hamamatsu silicon photomultiplier S10362-11-050C, Nucl. Instrum. Methods Phys. Res. A 762 (2014) 149–161, http://dx.doi.org/10.1016/j.nima.2014.05.112.

[7] M. Moll, Displacement damage in silicon detectors for high energy physics, IEEE Trans. Nucl. Sci. 65 (8) (2018) 1561–1582, http://dx.doi.org/10.1109/tns.2018.2819506.

[8] J.R. Srour, J.M. Mcgarrity, Radiation effects on microelectronics in space, Proc. IEEE 76 (11) (1988) 1443–1469.

[9] G.D. Watkins, Intrinsic defects in silicon, Mater. Sci. Semicond. Process. 3 (4) (2000) 227–235.

[10] E. Garutti, Y. Musienko, Radiation damage of SiPMs, Nucl. Instrum. Methods Phys. Res. A 926 (2019) 69–84, http://dx.doi.org/10.1016/j.nima.2018.10.191.

[11] O. Bychkova, P. Parygin, E. Garutti, A. Kaminsky, S. Martens, E. Popova, J. Schwandt, A. Stifutkin, Radiation hardness study using SiPMs with single-cell readout, Nucl. Instrum. Methods Phys. Res. A 1031 (2022) http://dx.doi.org/10.1016/j.nima.2022.166533.

[12] L. Mitchell, B. Phlips, W.N. Johnson, M. Johnson-Rambert, A.N. Kansky, R. Woolf, Radiation damage assessment of SensL SiPMs, Nucl. Instrum. Methods Phys. Res. A 988 (2021) http://dx.doi.org/10.1016/j.nima.2020.164798.

[13] Y. Musienko, D. Renker, Z. Charifoulline, K. Deiters, S. Reucroft, J. Swain, Study of radiation damage induced by 82MeV protons on multi-pixel Geiger-mode avalanche photodiodes, Nucl. Instrum. Methods Phys. Res. A 610 (1) (2009) 87–92, http://dx.doi.org/10.1016/j.nima.2009.05.052.

[14] Y. Li, X. Wen, X. Sun, X. Liu, X. Liang, D. Guo, W. Peng, K. Gong, G. Li, H. Wang, S. Xiong, J. Liao, H. Lu, J. Wang, Z. An, D. Zhang, M. Gao, G. Chen, Y. Liu, S. Yang, R. Qiao, F. Zhang, X. Zhao, Y. Xu, Y. Zhu, X. Li, The GECAM and its payload, Sci. Sinica Phys., Mech. Astron. 50 (12) (2020) http://dx.doi.org/10.1360/sspma-2019-0417.

[15] N. Hirade, H. Takahashi, N. Uchida, M. Ohno, K. Torigoe, Y. Fukazawa, T. Mizuno, H. Matake, K. Hirose, S. Hisadomi, K. Nakazawa, K. Yamaoka, N. Werner, J. Řípa, S. Hatori, K. Kume, S. Mizushima, Annealing of proton radiation damages in Si-PM at room temperature, Nucl. Instrum. Methods Phys. Res. A 986 (2021) http://dx.doi.org/10.1016/j.nima.2020.164673.

[16] K.D. Bartlett, D.D.S. Coupland, D.T. Beckman, K.E. Mesick, Proton irradiation damage and annealing effects in ON Semiconductor J-series silicon photomultipliers, Nucl. Instrum. Methods Phys. Res. A 969 (2020) http://dx.doi.org/10.1016/j.nima.2020.163957.

[17] H. Hofer ETH Zürich HansHofer, J.-L. Faure, D.-D. Saclay, J.-L. cernch, P.L. CERN, P. cernch, H. Rykaczewski, E.Z.H. cernch, F. Pauss, E. Zürich, The electromagnetic calorimeter technical design report CMS electromagnetic calorimeter project manager deputy project manager technical coordinator resource manager editor-in-chief, 1997.

[18] T. Tsang, Silicon photomultipliers radiation damage and recovery via high temperature annealing, J. Instrum. 13 (10) (2018) P10019, http://dx.doi.org/10.1088/1748-0221/13/10/p10019.

[19] M. Calvi, P. Carniti, C. Gotti, C. Matteuzzi, G. Pessina, Single photon detection with SiPMs irradiated up to 1014 cm-2 1-MeV-equivalent neutron fluence, Nucl. Instrum. Methods Phys. Res. A 922 (2019) 243–249, http://dx.doi.org/10.1016/j.nima.2019.01.013.

[20] J.G. Lim, E. Anisimova, B.L. Higgins, J.P. Bourgoin, T. Jennewein, V. Makarov, Laser annealing heals radiation damage in avalanche photodiodes, EPJ Quantum Technol. 4 (1) (2017) 11, http://dx.doi.org/10.1140/epjqt/s40507-017-0064-x.

[21] T. Tsang, T. Rao, S. Stoll, C. Woody, Neutron radiation damage and recovery studies of SiPMs, J. Instrum. 11 (12) (2016) P12002, http://dx.doi.org/10.1088/1748-0221/11/12/p12002.

[22] M. Cordelli, E. Diociaiuti, A. Ferrari, S. Miscetti, S. Müller, G. Pezzullo, I. Sarra, An induced annealing technique for SiPMs neutron radiation damage, J. Instrum. 16 (12) (2021) http://dx.doi.org/10.1088/1748-0221/16/12/t12012.

[23] H.M. Liu, Y. Peng, J.Y. Long, W.X. Lv, K. Liang, R. Yang, D.J. Han, A technique of in-situ annealing and temperature monitoring for silicon photomultipliers, in: 2019 IEEE Nuclear Science Symposium and Medical Imaging Conference (NSS/MIC), 2019, pp. 1–3, http://dx.doi.org/10.1109/NSS/MIC42101.2019.9059772.

[24] C. Leroy, P.-G. Rancoita, Particle interaction and displacement damage in silicon devices operated in radiation environments, Rep. Progr. Phys. 70 (4) (2007) 493–625, http://dx.doi.org/10.1088/0034-4885/70/4/r01.

[25] ONSEMI, Silicon Photomultiplier Sensors, J-Series (SiPM), URL https://www.onsemi.com/download/data-sheet/pdf/microj-series-d.pdf.

[26] HAMAMATSU, S14160-3010PS, URL https://www.hamamatsu.com/content/dam/hamamatsu-photonics/sites/documents/99_SALES_LIBRARY/ssd/s14160-1310ps_etc_kapd1070e.pdf.

[27] NDL, EQR15 Series SiPMs, URL http://www.ndl-sipm.net/PDF/Datasheet-EQR15.pdf.

[28] J.X. Yu, The IAE Peking HI-13 tandem accelerator, Nucl. Instrum. Methods 184 (1) (1981) 157–159.

[29] J.-Y. Tang, Q. An, J.-B. Bai, J. Bao, Y. Bao, P. Cao, H.-L. Chen, Q.-P. Chen, Y.-H. Chen, Z. Chen, Z.-Q. Cui, R.-R. Fan, C.-Q. Feng, K.-Q. Gao, X.-L. Gao, M.-H. Gu, C.-C. Han, Z.-J. Han, G.-Z. He, Y.-C. He, Y. Hong, Y.-W. Hu, H.-X. Huang, X.-R. Huang, H.-Y. Jiang, W. Jiang, Z.-J. Jiang, H.-T. Jing, L. Kang, B. Li, C. Li, J.-W. Li, Q. Li, X. Li, Y. Li, J. Liu, R. Liu, S.-B. Liu, X.-Y. Liu, Z. Long, G.-Y. Luan, C.-J. Ning, M.-C. Niu, B.-B. Qi, J. Ren, Z.-Z. Ren, X.-C. Ruan, Z.-H. Song, K. Sun, Z.-J. Sun, Z.-X. Tan, X.-Y. Tang, B.-B. Tian, L.-J. Wang, P.-C. Wang, Z.-H. Wang, Z.-W. Wen, X.-G. Wu, X. Wu, L.-K. Xie, X.-Y. Yang, Y.-W. Yang, H. Yi, L. Yu, T. Yu, Y.-J. Yu, G.-H. Zhang, L.-H. Zhang, Q.-W. Zhang, X.-P. Zhang, Y.-L. Zhang, Z.-Y. Zhang, L.-P. Zhou, Z.-H. Zhou, K.-J. Zhu, Back-n white neutron source at CSNS and its applications, Nucl. Sci. Tech. 32 (1) (2021) http://dx.doi.org/10.1007/s41365-021-00846-6.

[30] A. International, Standard practice for characterizing neutron fluence spectra in terms of an equivalent monoenergetic neutron fluence for radiation-hardness testing of electronics, 2019, URL https://www.astm.org/e0722-19.html.

[31] A.V.G. Lindstroem, Displacement damage in silicon, 2018, URL http://www.cern.ch/rd50/.

[32] A. Heering, Y. Musienko, J. Gonzales, A. Karneyeu, M. Wayne, R. Ruchti, M. Moll, Low temperature characteristics of SiPMs after very high neutron irradiation, Nucl. Instrum. Methods Phys. Res. A 936 (2019) 671–673, http://dx.doi.org/10.1016/j.nima.2018.09.111.

[33] P. Bohn, A. Clough, E. Hazen, A. Heering, J. Rohlf, J. Freeman, S. Los, E. Cascio, S. Kuleshov, Y. Musienko, C. Piemonte, Radiation damage studies of silicon photomultipliers, Nucl. Instrum. Methods Phys. Res. Sect. A 598 (3) (2009) 722–736, http://dx.doi.org/10.1016/j.nima.2008.10.027, URL<GotoISI>://WOS:000262825500010, 399ut Times Cited:28 Cited References Count:12.

[34] A. Heering, Y. Musienko, J. Gonzales, A. Karneyeu, M. Wayne, R. Ruchti, M. Moll, Low temperature characteristics of SiPMs after very high neutron irradiation, Nucl. Instrum. Methods Phys. Res. A 936 (2019) 671–673, http://dx.doi.org/10.1016/j.nima.2018.09.111.

[35] Z. Li, Y. Xu, C. Liu, Y. Gu, F. Xie, Y. Li, H. Hu, X. Zhou, X. Lu, X. Li, S. Zhang, Z. Chang, J. Zhang, Z. Xu, Y. Zhang, J. Zhao, Characterization of radiation damage caused by 23MeV protons in Multi-Pixel Photon Counter (MPPC), Nucl. Instrum. Methods Phys. Res. A 822 (2016) 63–70, http://dx.doi.org/10.1016/j.nima.2016.03.092.

[36] A. Ulyanov, D. Murphy, J. Mangan, V. Gupta, W. Hajdas, D. de Faoite, B. Shortt, L. Hanlon, S. McBreen, Radiation damage study of SensL J-series silicon photomultipliers using 101.4 MeV protons, Nucl. Instrum. Methods Phys. Res. A 976 (2020) http://dx.doi.org/10.1016/j.nima.2020.164203.

[37] M. Angelone, M. Pillon, R. Faccini, D. Pinci, W. Baldini, R. Calabrese, G. Cibinetto, A. Cotta Ramusino, R. Malaguti, M. Pozzati, Silicon photo-multiplier radiation hardness tests with a beam controlled neutron source, Nucl. Instrum. Methods Phys. Res. A 623 (3) (2010) 921–926, http://dx.doi.org/10.1016/j.nima.2010.07.057.

[38] I.V. Khodyuk, F.G.A. Quarati, M.S. Alekhin, P. Dorenbos, Energy resolution and related charge carrier mobility in LaBr3:Ce scintillators, J. Appl. Phys. 114 (12) (2013) http://dx.doi.org/10.1063/1.4823737.

[39] M. Ramilli, Characterization of SiPM: Temperature dependencies, 2008, http://dx.doi.org/10.1109/nssmic.2008.4774854.